Lagrangian Kinematic Criterion for the Breaking of Shoaling Waves

Uri Itay and Dan Liberzon

Faculty of Civil and Environmental Engineering, Technion–Israel Institute of Technology, Haifa, Israel

(Manuscript received 26 December 2016, in final form 6 March 2017)

ABSTRACT

An experimental study was conducted with the aim of validating the Lagrangian kinematic criterion (LKC) for the case of breaking of shoaling waves. Monochromatic wave trains were generated in a large wave flume and allowed to shoal and break naturally on an artificial inclination changeable shore, thus allowing inspection of a range of slopes. Instantaneous horizontal Lagrangian water surface velocity was measured by particle tracking velocimetry and compared to the instantaneous propagation speed of the crest on a verge of breaking, the latter calculated using time series produced by resistance-type wave gauges staged along the flume. The inception of a breaker was found to occur when the monotonically increasing horizontal water velocity on the crest, during the process of steepening, approached that of the slowing steep crest, thus confirming the LKC for shoaling conditions. In addition, an objective method of breaking detection was developed utilizing the phase–time method and wavelet analysis by recognizing a specific pattern in the instantaneous local frequency fluctuations. The two main expected contributions of this study are the formation of an applicable criterion for breaking occurrences in shoaling waves and development of a wave breaking detection method independent of human decision. Incorporation of the suggested criterion into existing waves prediction models can be a significant contribution to maritime projects efficiency, whereas the breakers detection method will be useful for conducting further experimental research on waves breaking both in laboratory installations and in the highly unstable environment of an open sea.

1. Introduction

The energy balance in the upper ocean is maintained partially due to the waves breaking. Part of the energy being transferred throughout the ocean surface is accumulated in steepening waves up to the point of breaking, followed by eventual energy dissipation and redistribution. Both the wind flow above and the water movement below are being affected by breaking waves; occurrence of breaking also leads to significantly magnified hydrodynamic loads on nearby objects (Melville and Rapp 1988). Therefore, a comprehensive understanding of the physical mechanisms governing waves breaking is essential for various scientific and engineering applications, such as sediment transport, impact on offshore infrastructure, and global aerosol mass transfer.

The highly irregular nature of waves breaking was in the focus of scientific research during the recent decades, the main goals being identification of the wave field conditions susceptible to frequent occurrence of breakers and determination of breaking criterion. The latter being a parameter that can be measured in the region of a wave crest and for which a threshold crossing would imply that the wave is breaking or about to break (Stansell and MacFarlane 2002). The highly nonlinear nature of steep and asymmetric waves on the verge of breaking renders the problem of interest as an analytically complex one, requiring thorough experimental examination. At the same time, the lack of an objective method for detection of breakers (besides whitecaps counting) and relying on human decision regarding the exact moment of the inception of breaking complicates the experimental research.

Through the last decades, progress has been made in numerous numerical and experimental studies of the topic, and various geometric, dynamic, and kinematic criteria for waves breaking have been suggested and examined. In recent studies, several reviews of suggested criteria were presented (e.g., Babanin 2011; Williams 1981; Stansell and MacFarlane 2002) and were found to be insufficient for various reasons, from reliance on linear theory to dependency on laboratory parameters not available in open seas. For a recent comprehensive review on this topic, see Perlin et al. (2013).

Corresponding author e-mail: Dan Liberzon, liberzon@technion.ac.il

DOI: 10.1175/JPO-D-16-0289.1

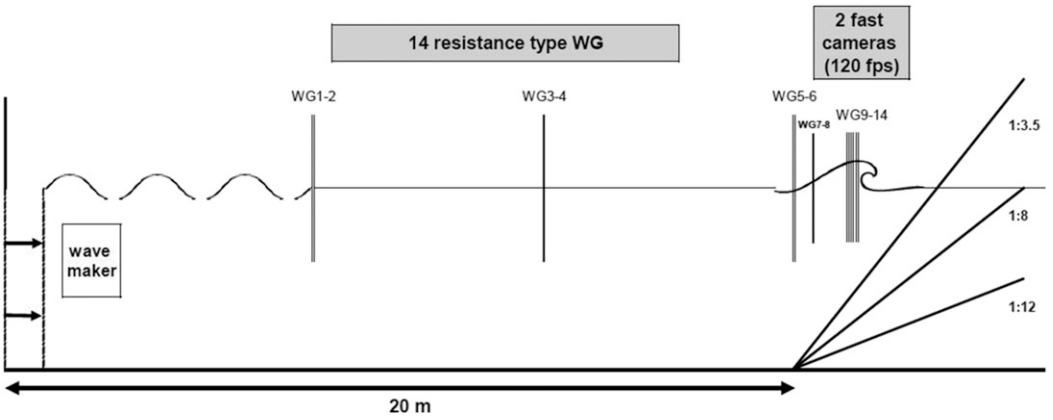

FIG. 1. Depiction of wave flume and measurement equipment.

So, an applicable universal criterion for breaking inception in the open sea is not yet available.

Using experimental methods based on a comparison of crest propagation speed with the directly measured Lagrangian water surface velocities at the wave's crest a Lagrangian kinematic criterion (LKC) was recently suggested and tested for deep-water spilling breakers (Shemer and Liberzon 2014). For this study, a particle tracking velocimetry (PTV) was used to obtain Lagrangian velocities of the water surface, while local crest propagation speed was obtained by a series of closely distributed wave gauges. The steep crest propagation speed was found to decrease simultaneously with a sharp increase in water surface velocity on the crest, the inception of breaking occurring when both approach equality. The slowdown of a crest propagation velocity of deep-water waves on the verge of breaking was also reported in Banner et al. (2014) based on numerical simulations and wave basin experiments.

Presenting a promising kinematic criterion, these studies are followed here by an experimental effort to verify an existence of the same LKC for naturally shoaling breakers. In addition, a new method for objective detection of breaking waves was developed based on a Phase–Time Method (PTM) originally proposed by Huang et al. (1992) and Zimmermann and Seymour (2002). The breaking events were found to be associated with a sharp increase of the instantaneous surface variations' frequency and to exhibit a specific pattern. Here we implement a wavelet analysis for pattern recognition, effectively allowing detection of breakers independently of human decision.

2. Experimental setup

This study has examined the validity of the Lagrangian kinematic breaking criterion introduced in Shemer and Liberzon (2014) for the case of shoaling breakers. Experimental measurements were staged in a large wave's flume (30 m long, 2.5 m wide, with water depth of 1 m) located at the Technion, Israel. Aiming to avoid artificial generation of nonlinear effects, short trains of deep-water monochromatic waves were generated 20 m away from an artificial rigid shore constructed for this purpose and were allowed to steepen and break naturally on the shore. The parameters for generation of monochromatic waves were chosen according to preliminary observations, aiming the breaking site to occur at least one wavelength from the beginning of shore slope. The waves generated by the piston-type wavemaker were hence about 1.5 m long at $H = 10$-cm wave height, resulting in deep-water wave steepness of roughly $ak = 0.2$, where a is the wave amplitude and k the wave number. To simulate a variety of shoaling processes, the artificial 6-m-long shore was constructed with changeable inclination angle, and measurements were carried out at three slope ratios of 1:12, 1:8, and 1:3.5. Important parameters of waves shoaling on the artificial beach were obtained using a combination of flow visualization techniques (PTV) and traditional resistance-type wave gauges.

Instantaneous surface elevation records were obtained at sampling frequency of 840 Hz by numerous resistance-type wave gauges positioned along the flume, as seen in Fig. 1: two pairs of gauges in deep water located at 8 and 14 m from wave generator, two pairs right before the shore and midway to the breaking site, and six additional wave gauges at the breaking site. Distance between each pair and between each of the six shore gauges was 5 cm. The high sampling frequency in combination with the dense array of the gauges at the shore allowed for a tight tracking of rapidly changing crest propagation velocity toward breaking, also providing a high-resolution data of the changing wave shape, used for the developing of a new breaking detection method.

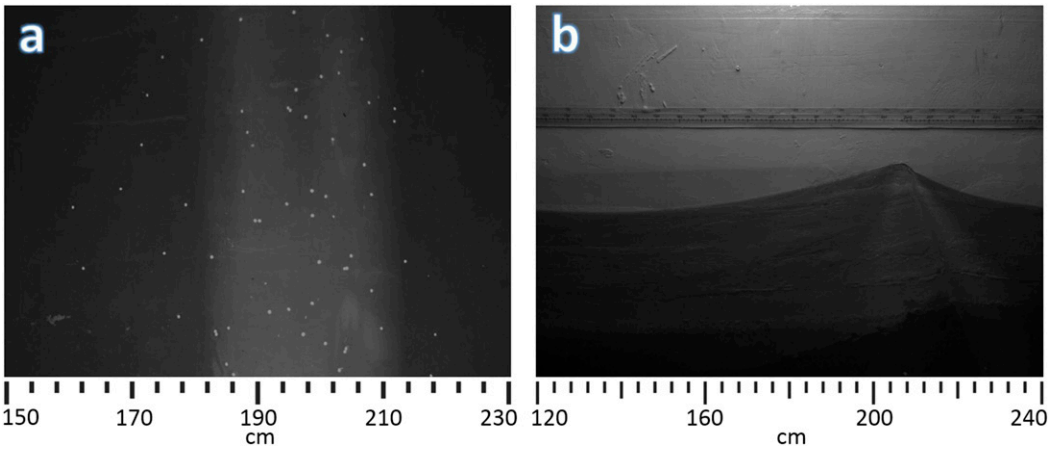

FIG. 2. Representative frames filmed by the two cameras showing (b) wave profile and (a) corresponding particles motion on the water surface. Rulers at the bottom of each frame indicate along the flume distance specified with respect to beginning of shore.

Visualization of the evolving and breaking waves was achieved by using two identical fast cameras mounted on a mobile instrument carriage. Both cameras provided synchronized video recordings at 4-megapixel resolution at the rate of 120 frames per second (fps). The first camera (Fig. 2a) was aimed vertically downward, recording the water surface area of 64 by 80 cm^2 with spatial resolution of 26 pixels cm^{-1}. The camera recorded movements of buoyant particles, 3 mm in diameter, seeded on the water surface. The recorded images sequences were then processed and water surface velocities u and v were obtained by PTV, utilizing the in-house developed MATLAB routine (Liberzon and Shemer 2011). The second camera was pointed toward the flume wall, recording fluctuations of the water surface in a 96 by 120 cm^2 area at 17 pixels cm^{-1} resolution (Fig. 2b) and was used to follow the changes in shoaling wave shape and to visually detect the inception of breaking. Both cameras' recordings were synchronized with the surface elevation fluctuations records obtained by the wave gauges, allowing accurate detection of the crest position in each frame and obtaining water surface velocities at the crest. A comparison of water surface velocity on the wave's crest (obtained by PTV), with the latter propagation speed (calculated using time series produced by wave gauges) up to and at the inception of a breaker has allowed the examination of the validity of the LKC for shoaling breakers.

3. Methods

Particles on the crest, namely, the ones relevant for the examination of the proposed LKC, were selected by tracking the crest's location using images acquired from the synchronized camera aimed toward the wall. A curve representing the wave profile on the wall in each frame was obtained by means of edge detection, allowing detection of the instantaneous crest location. A band of 4 cm around the specific location of the crest was then considered as the crest width and allowed selection of the relevant particles in PTV processing.

Measurement of various important waves' parameters such as height, steepness, and phase and group velocities were obtained from the records of instantaneous fluctuations of the water surface provided by several consecutive resistance-type wave gauges located along the flume. Steep crest propagation speed was measured using a densely spread six resistance-type wave gauges, positioned at 5-cm intervals along the shore, with X_{WG_i} denoting each wave gauge position. Waves' crests were tracked in each wave gauge record, pointing out six instants of the crest at the known wave gauges locations (T_{max_i}). The steep crest propagation speed u_c between each pair of wave gauges was then calculated by

$$u_c = \frac{X_{\mathrm{WG}_{i+1}} - X_{\mathrm{WG}_i}}{T_{\mathrm{max}_{i+1}} - T_{\mathrm{max}_i}}. \tag{1}$$

Wave gauges' data, in combination with the images of the instantaneous wave shape as recorded by the second camera, were also used for the developing of an objective method for breaking detection, based on the local frequency variations in the highly nonlinear wave. A PTM described in Zimmermann and Seymour (2002) was implemented to obtain records of instantaneous frequency fluctuations $F(t)$ from those of the surface elevation $\eta(t)$ as

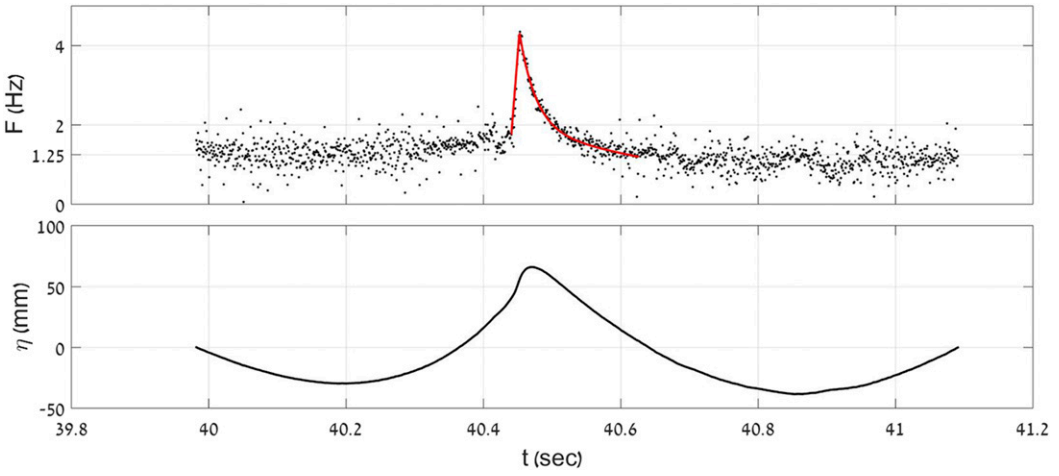

FIG. 3. (a) The pattern in the $F(t)$ signal associated with the inception of a breaker is marked by a solid red curve. A sharp, nearly linear rise in local frequency to the point of breaking followed by an exponential decay to the value of the carrier wave frequency is recognized. (b) The corresponding water elevation time series is presented.

$$F(t) = \frac{[\partial \upsilon(t)/\partial t]\eta(t) - [\partial \eta(t)/\partial t]\upsilon(t)}{\eta(t)^2 + \upsilon(t)^2}, \tag{2}$$

where $\upsilon(t)$ denotes the Hilbert transform of surface fluctuations

$$\eta(t) = \sum_{n=0}^{\infty} a_n \cos(n\sigma t) + b_n \sin(n\sigma t), \tag{3}$$

defined as

$$\upsilon(t) = \sum_{n=0}^{\infty} a_n \sin(n\sigma t) - b_n \cos(n\sigma t). \tag{4}$$

Here, a_n and b_n denote the harmonic components' coefficients, and σ is the angular frequency.

The PTM method was used by Zimmermann and Seymour (2002) and Irschik et al. (2010) to detect breaking events by associating the breaking inception with an increase in instantaneous frequency values, looking for a valid threshold. However, such an approach is limited as the threshold values of frequency vary significantly with basic parameters of each breaker. Here, a different approach is adopted, as inspection of the local frequency variations records have revealed a distinct pattern (Fig. 3) similar in form for all breakers associated with the moment of inception of breaker. Hence, a pattern recognition algorithm was developed to detect instances of such distinct patterns in records of $F(t)$. The sought after pattern consisted of a sharply rising linear part corresponding the leading face of a breaking wave followed by an exponential decay corresponding the back of the wave. The automatic detection of such patterns in $F(t)$ was achieved by constructing an adapted wavelet of a similar form and then processing the full $F(t)$ record with this wavelet. The exact moment of breaking inception was determined to be when the wavelet analysis signal energy reached its maximum, indicating the best matching of the pattern in the signal. Discussion of the automatic breaking inception results is given later in the text.

The experiment order included first setting a desired shore slope and performance of preliminary trials of different wave parameters until a distinct breaking occurs at least one wavelength into the shore region. After a set of wave parameters is selected, all measurement instruments were aligned at the relevant location of breaking. Then the fine tuning of cameras' regions of interest and lighting conditions, and achieving satisfactory particles seeding density and scatter, were performed. Small variations in waves shoaling behavior, as the waves were allowed to evolve and break naturally, caused small variations in the actual location of the inception of breaker. Numerous runs were hence required to produce repetitive breaking location and satisfactory quality of records of breakers. Eventually four to seven breaking events were recorded and processed at each inclination, and the results are elaborated below.

4. Results and discussion

Figure 4 presents the data processing results of all breaking events as recorded at each inclination examined. The figure presents, for each slope, an ensemble of PTV-obtained water surface velocity u at the crest versus the crest propagation velocity u_c obtained from the wave gauges records. Values of $u = \sigma H/2$ and celerity calculated from linear theory for both deep- and shallow-water

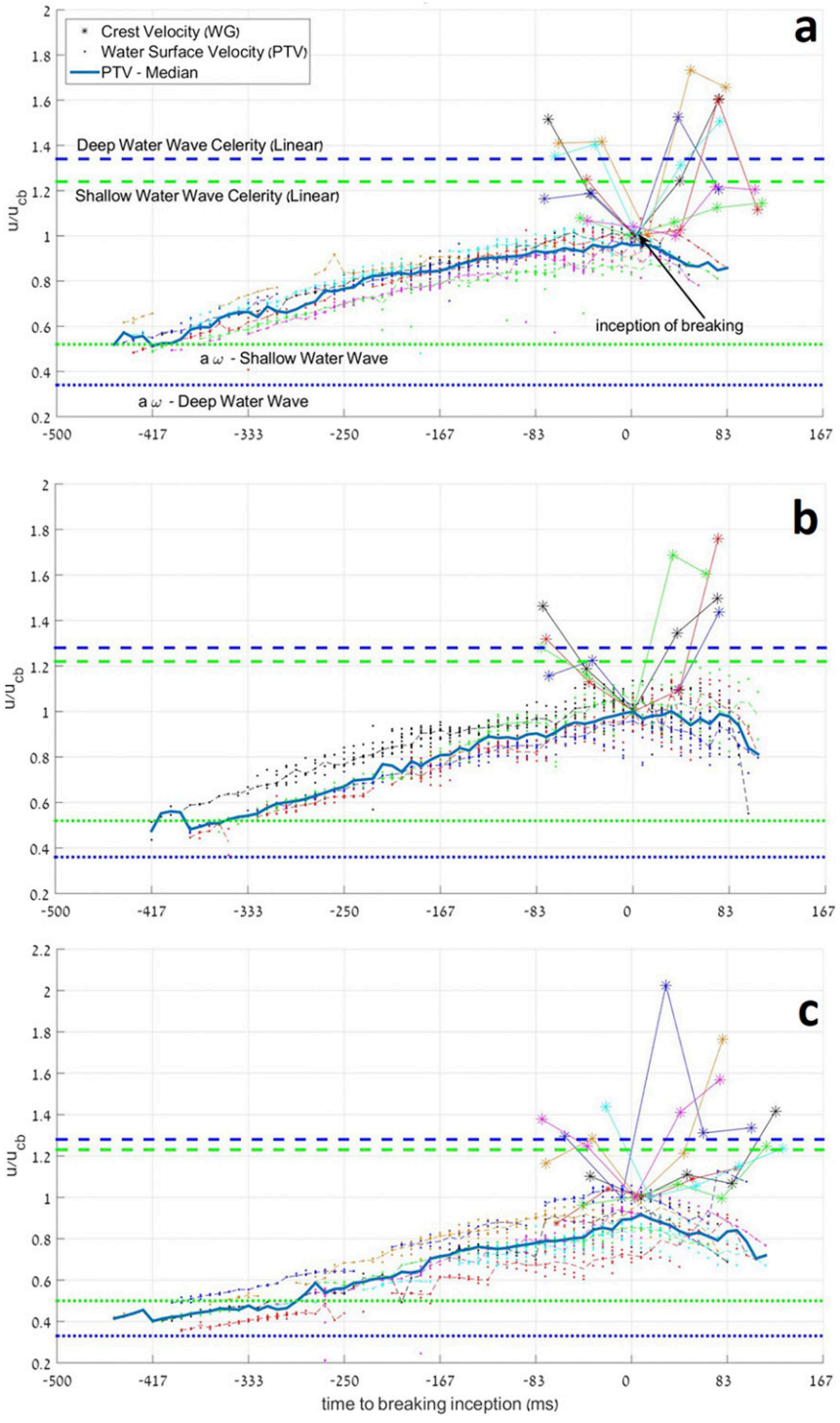

FIG. 4. Results from each of the examined slopes: (a) 1:3.5; (b) 1:8; (c) 1:12. Each dot in the PTV obtained Lagrangian water surface velocity ensemble denotes an instantaneous velocity of a specific buoyant particle. The number of colors is the same as the number of successful experiments. The solid blue curve represents the median value of the ensemble. Colored stars denote the corresponding crest propagation velocities as obtained from wave gauges' records, the instantaneous values are connected by lines of the same color for the better visualizing of changes. For reference, values of linear water velocity at the crest and wave celerity for deep- and shallow-water cases are also presented. All velocities are normalized to the crest propagation velocity at the inception of a breaker u_{cb}.

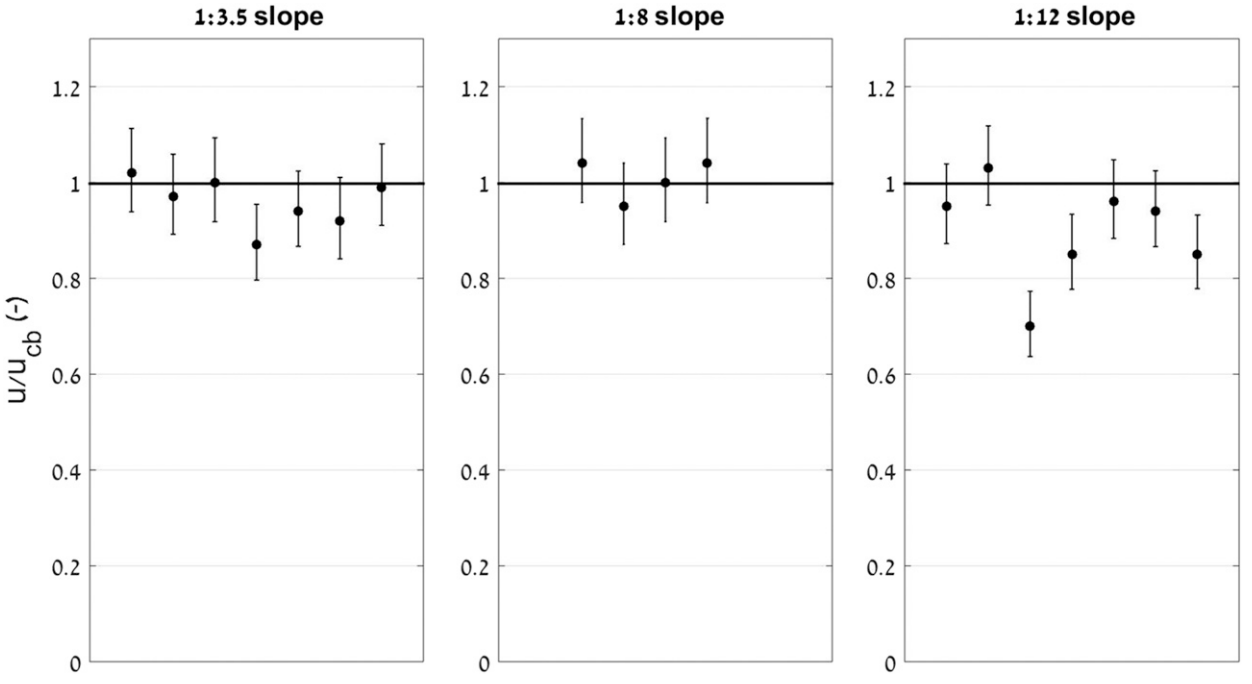

FIG. 5. Summary of the results at all three slope ratios, presented as the ratio between u (Lagrangian water velocity on the crest at the inception of breaking) and u_{cb} (crest propagation velocity at the inception of breaking).

waves of similar time period and depth of breaking are also given for the sake of reference. All velocities are normalized with respect to crest velocity at the inception of breaking u_{cb}, and the time axis is shifted so $t = 0$ represents the instant of breaking as detected by visual observations of the wave form in the second camera records. The results demonstrate a slowdown of crest propagation accompanied by an increase in water surface velocity on the crest as the wave approaches the inception of breaking. These are in agreement with near-breaking behavior observed by Shemer and Liberzon (2014) and in Banner et al. (2014) in deep-water waves, in which the crest slowdown was explained by slow developing of wave group envelope and by the interplay between the nonlinearities and dispersion, whereas in the current experiments the shoaling effect should also contribute to the observed crest slowdown. Both velocities' values are approaching equality toward the inception of breaking, a behavior detected at all three examined shore slope ratios. Figure 5 summarizes the results, presenting values of the u/u_{cb} ratio at the inception of breaking.

Overall, the ratio between the Lagrangian surface velocity u and the steep crest propagation velocity u_{cb} ranges between 0.85 and 1.04 at the inception of breaking in all examined experiments and may practically point that for the present circumstances equality exists at the inception of breaking, given the size of depicted error bars. Error bars of the obtained velocities were calculated considering typical length and time inaccuracies of the measuring instruments involved. In crest propagation velocities the errors originated mainly from the width of the wave gauges' rods being 4 mm in diameter. The accuracy of PTV-obtained particles velocities depends mainly on particles position detection in each frame. Taking into consideration the spatial resolution of the images and the particles' diameter of 3 mm, the error here was evaluated to be 2 pixels, allowing an average error of 25% of particles size.

Last, the performance of a new method, independent of human decision, for detection of breakers was examined. Comparison of human observation based and the automated method detection of the inception of breaking is shown in Fig. 6. The results are presented in the form of time differences of the detected moment of inception as obtained by the two methods. Most of time differences are around 50 ms, presenting an outstanding accuracy of the proposed method for detection of breakers.

To conclude, the experiments presented here verify the validity of the LKC for the examined cases of shoaling breakers on three slope ratios, within the limitations of presented experimental setup. The prospects of the LKC validation for additional cases of breakers need to be examined by staging additional experiments and eventually researching the validity of LKC for breakers in random waves' fields and waves' fields under wind forcing. To assist conducting such complex experiments in the future, a new objective method for detection of

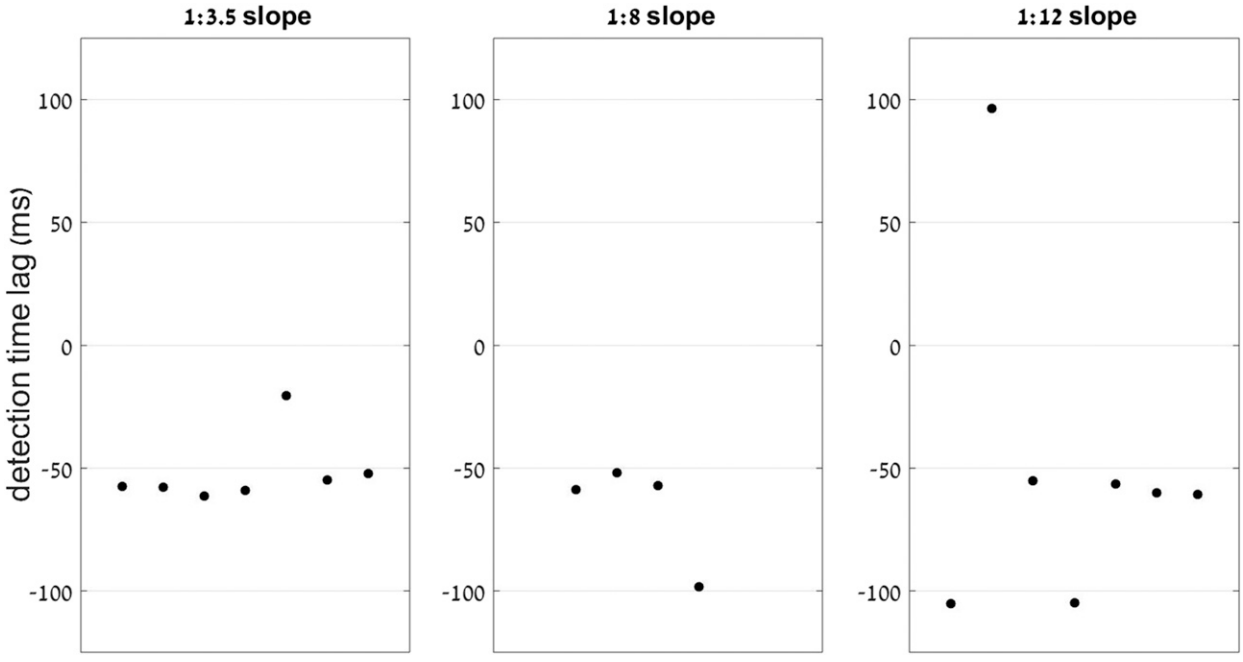

FIG. 6. PTM vs human observation detection of breaking inception, with 0 marking the time of detection by human observation.

breakers was developed based on detecting specific patterns associated with the inception of breaking in the instantaneous frequency variations records as obtained by PTM. The developed breaking detection method itself requires further thorough verification, since the results presented so far depend on the specific conditions of the conducted experiment, including monochromatic waves (initially), spilling breakers, and shoaling conditions. Furthermore, the results were achieved by the choice of a specific time window of three wave periods around the inception of a breaker in order to minimize the effect of irrelevant signal noise. The here suggested method of independent automatic detection may become a very useful tool in the fields of water waves' research and engineering, and it is recommended to keep examining its performance in other experimental conditions, such as plunging breakers. Implementation of this method will greatly contribute to the experimental research enabling better quantification of breaking events even in highly irregular fields under wind forcing.

Acknowledgments. We greatly appreciate the financial support provided for this research by the Israel Science Foundation Grant 1521/15.

REFERENCES

Babanin, A. V., 2011: *Breaking and Dissipation of Ocean Surface Waves*. Cambridge University Press, 463 pp., doi:10.1017/CBO9780511736162.

Banner, M. L., X. Barthelemy, F. Fedele, M. Allis, A. Benetazzo, F. Dias, and W. L. Peirson, 2014: Linking reduced breaking crest speeds to unsteady nonlinear water wave group behavior. *Phys. Rev. Lett.*, **112**, 114502, doi:10.1103/PhysRevLett.112.114502.

Huang, N. E., S. R. Long, C. Tung, M. A. Donelan, Y. Yuan, and R. J. Lai, 1992: The local properties of ocean surface waves by the phase-time method. *Geophys. Res. Lett.*, **19**, 685–688, doi:10.1029/92GL00670.

Irschik, K., S. Schimmels, and H. Oumeraci, 2010: Breaking Criteria for laboratory experiments based on the Phase-Time-Method (PTM). *Proc. 32nd Int. Conf. Coastal Engineering*, Shanghai, China, Coastal Engineering Research Council, 1–15, doi:10.9753/icce.v32.waves.6.

Liberzon, D., and L. Shemer, 2011: Experimental study of the initial stages of wind waves' spatial evolution. *J. Fluid Mech.*, **681**, 462–498, doi:10.1017/jfm.2011.208.

Melville, W. K., and R. J. Rapp, 1988: The surface velocity field in steep and breaking waves. *J. Fluid Mech.*, **189**, 1–22, doi:10.1017/S0022112088000898.

Perlin, M., W. Choi, and Z. Tian, 2013: Breaking waves in deep and intermediate waters. *Annu. Rev. Fluid Mech.*, **45**, 115–145, doi:10.1146/annurev-fluid-011212-140721.

Shemer, L., and D. Liberzon, 2014: Lagrangian kinematics of steep waves up to the inception of a spilling breaker. *Phys. Fluids*, **26**, 016601, doi:10.1063/1.4860235.

Stansell, P., and C. MacFarlane, 2002: Experimental investigation of wave breaking criteria based on wave phase speeds. *J. Phys. Oceanogr.*, **32**, 1269–1283, doi:10.1175/1520-0485(2002)032<1269:EIOWBC>2.0.CO;2.

Williams, J. M., 1981: Limiting gravity waves in water of finite depth. *Philos. Trans. Roy. Soc. London*, **A302**, 139–188. [Available online at http://www.jstor.org/stable/36960.]

Zimmermann, C.-A., and R. Seymour, 2002: Detection of breaking in a deep water wave record. *J. Waterw. Port Coastal Ocean Eng.*, **128**, 72–78, doi:10.1061/(ASCE)0733-950X(2002)128:2(72).